Electron-Phonon Interaction and Charge Carrier Mass Enhancement in $SrTiO_3$

J. L. M. van Mechelen,[1] D. van der Marel,[1] C. Grimaldi,[1,2] A. B. Kuzmenko,[1] N. P. Armitage,[1,3] N. Reyren,[1] H. Hagemann,[4] and I. I. Mazin[5]

[1]*Département de Physique de la Matière Condensée, Université de Genève, Genève, Switzerland*
[2]*LPM, Ecole Polytechnique Fédérale de Lausanne, Lausanne, Switzerland*
[3]*Department of Physics and Astronomy, The Johns Hopkins University, Baltimore, Maryland 21218, USA*
[4]*Département de Chimie Physique, Université de Genève, Genève, Switzerland*
[5]*Center for Computational Materials Science, Naval Research Laboratory, Washington, D.C. 20375, USA*

(Received 5 April 2007; revised manuscript received 15 April 2008; published 6 June 2008)

We report a comprehensive THz, infrared and optical study of Nb-doped $SrTiO_3$ as well as dc conductivity and Hall effect measurements. Our THz spectra at 7 K show the presence of an unusually narrow (< 2 meV) Drude peak. For all carrier concentrations the Drude spectral weight shows a factor of three mass enhancement relative to the effective mass in the local density approximation, whereas the spectral weight contained in the incoherent midinfrared response indicates that the mass enhancement is at least a factor two. We find no evidence of a particularly large electron-phonon coupling that would result in small polaron formation.

DOI: 10.1103/PhysRevLett.100.226403 PACS numbers: 71.38.−k, 72.20.−i, 78.20.−e

Electron-phonon coupling in the perovskites is a subject of much recent interest due to the controversy over its relevance in the phenomena of multiferroicity, ferroelectricity, superconductivity, and colossal magnetoresistance [1–5]. Despite much progress, full understanding of the physics of electron-phonon coupling in perovskites is still lacking because of additional crystallographic complexities of many materials involved (breathing, tilting and rotational distortions, ferroelectric symmetry breaking), magnetism, complex electronic effects (strong correlations), and also because of the lack of high-accuracy spectroscopic measurements specifically designed to probe electron-phonon coupling.

With this in mind, we have studied a prototypical perovskite oxide, $SrTi_{1-x}Nb_xO_3$ with $0 \leq x \leq 0.02$. $SrTiO_3$ is an insulator ($\Delta = 3.25$ eV) with the conduction band formed by the Ti $3d$ states. These are split by the crystal field so that the three t_{2g} states become occupied when the material is electron doped by substituting pentavalent Nb for tetravalent Ti. For $0.0005 \leq x \leq 0.02$ $SrTi_{1-x}Nb_xO_3$ becomes superconducting at a T_c of typically $\sim$0.3 K [6], and at most 1.2 K [5]. Characterized by the threefold degeneracy of the conduction bands and the high lattice polarizability, electron-doped $SrTiO_3$ provides a perfect opportunity for the study of electron-phonon coupling and polaron formation in an archetypal perovskite [7,8].

One of the fingerprints of an ultrastrong electron-phonon coupling is the formation of small polarons, which is observable in the form of a gigantic electron mass renormalization. The renormalized mass can be obtained by measuring the optical spectral weight of the Drude peak, which is equal to $\pi n e^2/(2m^*)$. Besides renormalizing the ''coherent'' (Drude) part of the spectrum, the electron-phonon coupling is responsible for ''incoherent'' contributions at higher energies, resulting in multiphonon absorption bands in the midinfared range.

To address these issues, we have measured the optical reflectivity and transmission of double side polished, 5×5 mm^2 [(100) face] single crystals of $SrTi_{1-x}Nb_xO_3$ between 300 K and 7 K by time-domain THz spectroscopy (TPI spectra 1000, TeraView Ltd.), Fourier transform infrared spectroscopy, and photometric IR-UV spectroscopy, in the range from 0.3 meV to 7 eV. To obtain a detectable transmission, we have used for each composition several samples of different thicknesses (8–60 μm), adopted to the spectral range and value of the optical transmission. The Hall carrier concentrations were 0.105%, 0.196%, 0.875%, and 2.00% at 7 K, which were within 5% of those measured by the wavelength-dispersive x-ray spectroscopy, and within 12% of the Nb concentration specified by the supplier (0.1%, 0.2%, 1.0%, and 2.0%, respectively, Crystec, Berlin). Compared to earlier measurements [9–13], we expand the lower limit of the spectral range from 1.2 meV [11] to 0.3 meV. The real and imaginary part of $\epsilon = \epsilon' + (4\pi/\omega)i\sigma_1$ were obtained from inversion of the Fresnel equations of transmission and phase (below 12 meV for the samples with $x = 0.001$ and 0.002), from inversion of the Fresnel equations of reflection and transmission coefficients (above 0.1 eV), and from Kramers-Kronig analyses of the reflectivity spectra (2–80 meV) with Drude-Lorentz fits [14] to aforementioned reflectivity, transmission, and phase spectra up to 7 eV, and ρ_{dc}.

The gap of $SrTiO_3$ is revealed as the sharp onset of the optical conductivity at 3.3 eV in all samples (Fig. 1). The absorption peak at 2.4 eV, with intensity proportional to the charge carrier density, reveals optical excitation of the doped t_{2g} states to the empty e_g states. The only subgap contributions to the optical conductivity of undoped $SrTiO_3$ (Fig. 1) are the three infrared active phonons at 11.0, 21.8, and 67.6 meV (at room temperature). The lowest one exhibits a strong redshift upon cooling, and saturates at about 2.3 meV at 7 K. Upon doping this mode

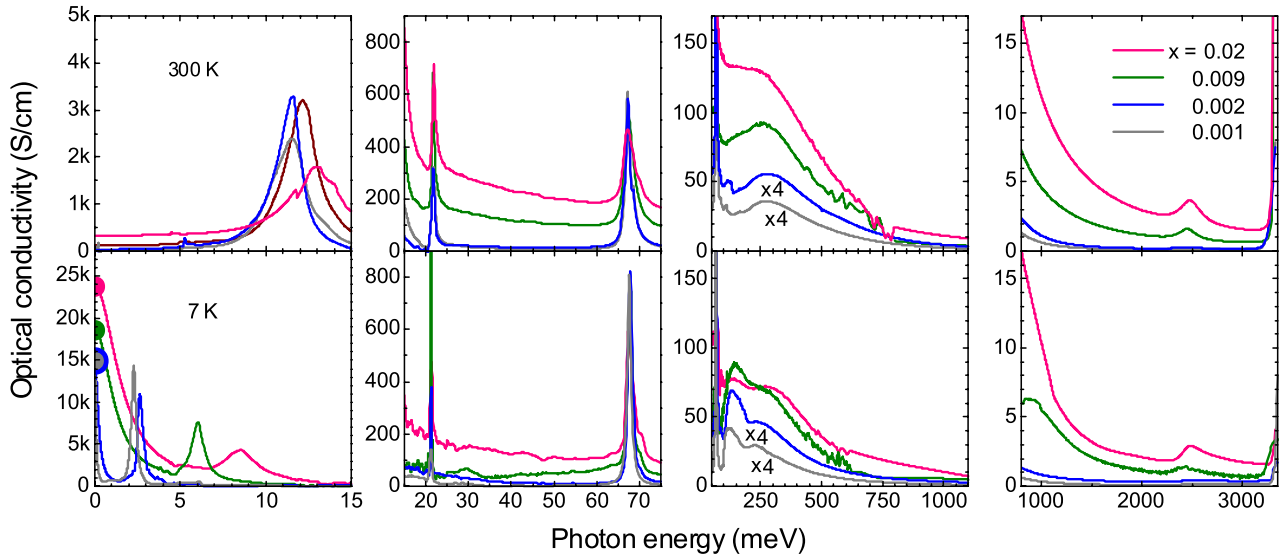

FIG. 1 (color online). The optical conductivity of $SrTi_{1-x}Nb_xO_3$ for $x = 0.001$, 0.002, 0.009, and 0.02 at 300 K (top) and 7 K (bottom), together with the dc conductivity (dots). For clarity the spectral windows corresponding to the extreme infrared, far-infrared, midinfrared, and visible ranges are displayed with different magnifications.

hardens for all temperatures, reaching 8.5 meV at 7 K at 2% doping. For the present discussion, the most important effect of substituting Nb is to dope electrons, which yields a clearly distinguishable Drude peak, which is broad at 300 K but gets extremely narrow (<2 meV) at low temperatures, as shown in Fig. 1. This unusually narrow Drude peak is the coherent part of the polaronic conduction in n-doped $SrTiO_3$ as will be argued below. For the 0.9% and 2% doped samples, the metallic conductivity is directly visible from the increase of the reflectivity below the soft optical phonon (see Ref. [15]). In addition, we observe a broad asymmetric midinfrared absorption, which increases with doping, confirming the result of Calvani *et al.* [9]. This band evolves into a double peak structure when the temperature is lowered to 7 K (Fig. 1). Using first principles local-density approximation (LDA) calculations [16], we have verified that interband transitions within the t_{2g} manifold are orders of magnitude too weak to account for the observed intensity. We will argue below that the observed line shape can be understood as a multiphonon sideband of the free carrier (Drude) response.

As mentioned before, the effective mass of the charge carriers m^* can be obtained by analyzing the Drude spectral weight. In Fig. 2 we show the spectral weight $W(\omega)$, defined as

$$W(\omega_c) \equiv \int_0^{\omega_c} \sigma_1(\omega) d\omega. \qquad (1)$$

The electronic contribution $8W(\infty) = \omega_p^2 = 4\pi ne^2/m$, where e and m are the free electron charge and mass, and n is the electron density. The contribution of the infrared phonons manifests itself in $W(\omega)$ as steps, e.g., at 8.5 meV in the 2% doped sample (Fig. 2). Such a strong phonon close to the Drude peak requires experimental data that extend beyond the soft phonon frequency. (i) The $\epsilon_1(\omega)$ and $\epsilon_2(\omega)$ data below 3 meV measured by time-domain THz spectroscopy (for $x = 0.001$ and 0.002) and (ii) far-infrared reflectivity (above 2 meV for $x = 0.001$ and 0.002, and above 4 meV for $x = 0.009$ and 0.02) are crucial for the separation of the spectral weight in the Drude peak from the large contribution by the soft phonon mode. This is particularly important for the lower doped samples, where the Drude spectral weight is one order of magnitude smaller than the spectral weight of the soft optical mode.

For the two lowest dopings we apply the partial sum rule [Eq. (1)] with cutoff frequencies $\hbar\omega_c = 1.5$ meV (0.1%) and 2.0 meV (0.2%), which are larger than the Drude relaxation rate but below the soft phonon (see Fig. 1) [19], yielding $\hbar\omega_p = 116 \pm 18$ meV and 159 ± 23 meV, $\hbar\omega_p = 412 \pm 53$ meV and 527 ± 61 meV for the samples

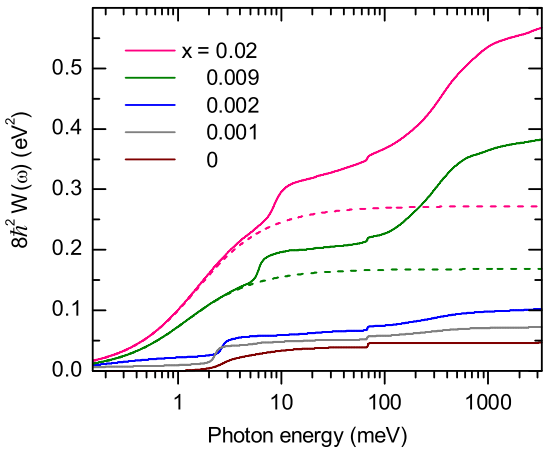

FIG. 2 (color online). The integrated optical spectral weight of $SrTi_{1-x}Nb_xO_3$ as a function of photon energy and relative to the charge carrier concentration, at 7 K. The Drude spectral weight is separately shown for $x = 0.9\%$ and $x = 2\%$ (dashed lines).

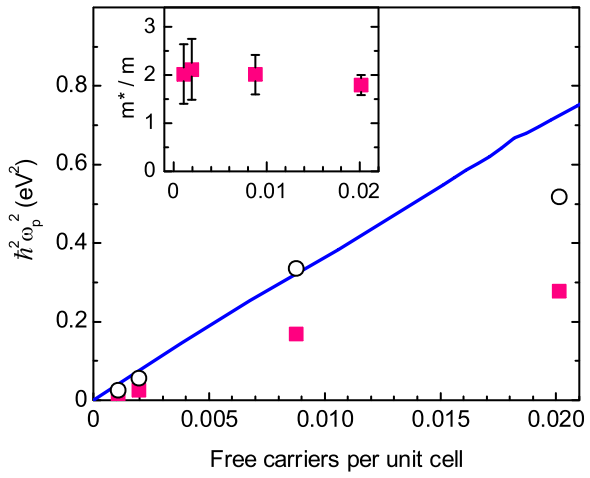

FIG. 3 (color online). Experimental plasma frequency at 7 K derived from the spectral weight of the Drude peak (squares) together with that from the band-structure calculations [16] (solid line) as a function of the free carrier concentration (from Hall effect). The circles display the total electronic spectral weight at 3 eV. The inset shows the corresponding effective carrier mass $m^*/m = (W_{\mathrm{mir}} + W_{\mathrm{Drude}})/W_{\mathrm{Drude}}$.

with $x = 0.001, 0.002, 0.009$, and 0.02, respectively, shown by the red squares in Fig. 3. Defining the mass renormalization of the charge carriers as the ratio of the total electronic spectral weight at 3 eV, W_{total}, and the Drude spectral weight, W_{Drude}, $m^*/m = W_{\mathrm{total}}/W_{\mathrm{Drude}}$, we observe a twofold mass enhancement, i.e., $m^*/m = 2.0 \pm 0.3$ for the low charge carrier densities considered in the present study (Fig. 3, inset). The calculated LDA band mass $m_b \approx 0.63 m_e$, which implies $m^*/m_b = 3.0 \pm 0.4$.

For $0.001 \leq x \leq 0.02$, the band-structure value [16] of the Fermi energy, E_F, ranges from 0.02 to 0.1 eV, relative to the bottom of the lowest t_{2g} band, which coincides with the energy of the relevant longitudinal optical phonon, $\hbar\omega_{\mathrm{LO}} = 0.1$ eV [20,21]. This is a difficult parameter range to describe theoretically where none of the usual approximations, i.e., $\hbar\omega_{\mathrm{LO}}/E_F \ll 1$ nor $\hbar\omega_{\mathrm{LO}}/E_F \gg 1$, are applicable. For the present discussion we consider the latter limit, appropriate for the lower doped samples. It takes as a starting point the model of a single polaron [22,23], characterized by the coupling constant α. Within a variational approximation, Feynman [22] deduced the relation $m^*(\alpha)$ valid in the range $0 < \alpha < 12$. Applying Feynman's relation to the experimental m^* values, we obtain a doping independent value $3 < \alpha < 4$, in excellent agreement with the value $\alpha = 3.6$ from the Fröhlich model in a polar medium with multiple optical phonon branches [24].

The optical conductivity shows a broad absorption band between 0.1 and 1 eV (Fig. 1). The f-sum rule, $8W(\infty) = \omega_p^2$, is almost satisfied at 3 eV (Fig. 3), demonstrating that the intensity in this midinfrared band compensates to a large extent the deficit of Drude spectral weight. Such spectral weight redistribution between the "coherent" (Drude) and the "incoherent" (midinfrared) contributions of the optical conductivity suggests that the mass enhancement reflects coupling of electrons to bosonic degrees of freedom, most probably phonons. A spectral shape similar to the observed midinfrared band at 300 K (Fig. 1) was calculated by Emin [25], who considered the photoionization spectrum out of the potential well formed by the lattice deformation of the polaron. Upon cooling, the maximum of this band remains between 200 and 350 meV, and at 7 K an additional peak emerges on the low-energy side with a maximum varying from 120 (0.1%) to 140 meV (2%). Devreese *et al.* [26,27] have numerically found a broad midinfrared band with (for intermediate couplings) a peak at lower energies. They explain it as a multiphonon band and the peak as a relaxed state of an electron optically excited within the polaronic potential well. The model predicts the maxima of the two bands to be at $0.065\alpha^2\hbar\omega_{\mathrm{LO}}$ and $0.14\alpha^2\hbar\omega_{\mathrm{LO}}$. With $\alpha \approx 4$ this corresponds to 110 meV and 230 meV, consistent with the experimentally observed positions (Fig. 1).

Figure 4 shows the temperature dependence of the spectral weight of both the Drude peak and the midinfrared band. Upon increasing temperature, our data show an increase of the midinfrared spectral weight, as earlier observed by Ref. [9], and a decrease of the same amount of Drude spectral weight, contrary to the expectation that thermal fluctuations undo the self-trapping and reduce the effective mass [28,29]. Kabanov and Ray explained this with a two-fluid model of delocalized carriers and localized polarons pinned to impurity sites [30]. However, in this model the Hall coefficient depends strongly on temperature and becomes completely suppressed at low temperatures, in contradiction to the almost constant Hall coefficient of our Nb-doped $SrTiO_3$ crystals [15]. While Ciuchi *et al.* [31] have demonstrated that the polaron radius *decreases* when the temperature is increased, the authors maintain that the polaron mass will decrease with increas-

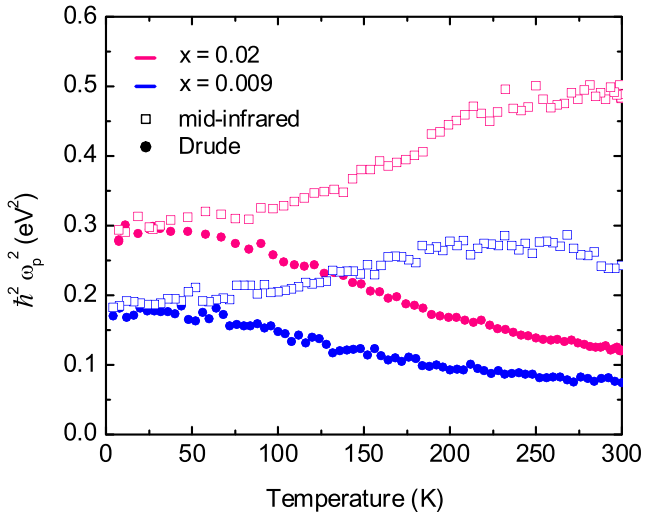

FIG. 4 (color online). Experimental temperature dependence of the spectral weight of both the Drude peak (circles) and the midinfrared band (squares) for $x = 2.0\%$ and $x = 0.9\%$.

ing temperature. Theoretical work until now has concentrated on the properties of a single polaron, while the important (but quite difficult) problem of the polaron liquid remains to be solved. In this respect we conjecture that in its ground state the electron-phonon interacting system forms a homogeneous fluid, which is uniformly accelerated by an external electric field, without excitation of the vibrational degrees of freedom. Since the charge fluid is no longer uniform at finite T due to thermal charge density excitations, its translation upon applying an electric field becomes increasingly hindered by coupling to the lattice vibrations when we increase the temperature, resulting in a reduced Drude spectral weight and an increase of the midinfrared spectral weight. The relevant temperature scale for this to occur is the Fermi temperature, less than 1000 K for the highest doped sample. The aforementioned process whereby a polaron will escape from its self-trapped potential will occur on the (higher) energy scale of the polaron binding energy, i.e., approximately 2000 K.

In conclusion, we observe an unusually narrow Drude peak in electron-doped $SrTiO_3$ at 7 K for charge carrier concentrations between 0.1% and 2% per unit cell, which is less than 1 meV for the lowest dopings. The suppression of the Drude spectral weight reveals a mass enhancement between two and three, which is caused by the electron-phonon coupling. The missing spectral weight is recovered in a series of midinfrared sidebands resulting from the electron-phonon coupling interaction, traditionally associated with the polaronic nature of the charge carriers. The effective mass yields an intermediate electron-phonon coupling strength, $3 < \alpha < 4$, thus suggesting that the charge transport in electron-doped $SrTiO_3$ is carried by large polarons. Increasing the temperature depletes further the Drude spectral weight, corresponding to an increase of the free carrier mass. This behavior, which is opposite to that of an isolated polaron, may signal that the low-temperature state of matter is a polaron liquid.

This work was supported by the Swiss National Science Foundation through the NCCR "Materials with Novel Electronic Properties" (MaNEP). We gratefully acknowledge stimulating discussions with J.-M. Triscone, K. S. Takahashi, T. Giamarchi, J. T. Devreese, J. Lorenzana, and Ø. Fischer.

[1] A. Lanzara *et al.*, Nature (London) **412**, 510 (2001).
[2] A. S. Alexandrov, J. Phys. Condens. Matter **19**, 125216 (2007).
[3] H. Y. Hwang, S.-W. Cheong, P. G. Radaelli, M. Marezio, and B. Batlogg, Phys. Rev. Lett. **75**, 914 (1995).
[4] N. Mannella *et al.*, Nature (London) **438**, 474 (2005).
[5] J. G. Bednorz and K. A. Müller, Rev. Mod. Phys. **60**, 585 (1988).
[6] C. S. Koonce, M. L. Cohen, J. F. Schooley, W. R. Hosler, and E. R. Pfeiffer, Phys. Rev. **163**, 380 (1967).
[7] P. Calvani, Riv. Nuovo Cimento Soc. Ital. Fis. **24**, 1-71 (2001).
[8] D. M. Eagles, M. Georgiev, and P. C. Petrova, Phys. Rev. B **54**, 22 (1996).
[9] P. Calvani, Phys. Rev. B **47**, 8917 (1993).
[10] D. A. Crandles, Phys. Rev. B **59**, 12842 (1999).
[11] F. Gervais, J.-L. Servoin, A. Baratoff, J. G. Bednorz, and G. Binnig, Phys. Rev. B **47**, 8187 (1993).
[12] A. S. Barker, Jr., *Optical Properties and Electronic Structure of Metals and Alloys*, edited by F. Abelès (North-Holland, Amsterdam, 1965), pp. 452–468.
[13] C. Z. Bi *et al.*, J. Phys. Condens. Matter **18**, 2553 (2006).
[14] A. B. Kuzmenko, Rev. Sci. Instrum. **76**, 083108 (2005).
[15] J. L. M. van Mechelen *et al.* (to be published).
[16] We employed the linear augmented plane wave method as implemented in the WIEN2K code (Karlheinz Schwarz, Techn. Universität Wien, Austria, 2001) and the generalized gradient approximation for the exchange-correlation potential in the form proposed by J. P. Perdew, K. Burke, and M. Ernzerhof [Phys. Rev. Lett. **77**, 3865 (1996)]. Calculations have been performed in the high-temperature perovskite structure ($a = 3.905$ Å) as well as in the low-temperature tetragonal structure (group No. 140, $I4/mcm$, $a = 5.529$ Å, $c = 7.824$ Å, $O_x = 0.244\%$). Optimizing the O position in the calculations yields $O_x = 0.223$. Nb doping was simulated by changing the nuclear charge of Ti from 22 to $22 + x$, or that of Sr from 38 to $38 + x$. Fermi-surface integrals were evaluated using the k-point meshes up to $28 \times 28 \times 28$. Our first principles results show a substantially weaker effect of the tetragonality compared to the semiempirical calculations of Mattheiss [17] (less than 4 meV splitting of the otherwise degenerate states at Γ, compared to $\sim$20 meV). This, in fact, resolves a long-standing controversy between the band structure of Ref. [17] and the de Haas–van Alphen measurements of Gregory *et al.* [18].
[17] L. F. Mattheiss, Phys. Rev. B **6**, 4740 (1972).
[18] B. Gregory, J. Arthur, and G. Seidel, Phys. Rev. B **19**, 1039 (1979).
[19] A. B. Kuzmenko, D. van der Marel, F. Carbone, and F. Marsiglio, New J. Phys. **9**, 229 (2007).
[20] J.-L. Servoin, Y. Luspin, and F. Gervais, Phys. Rev. B **22**, 5501 (1980).
[21] G. Verbist, F. M. Peeters, and J. T. Devreese, Ferroelectrics **130**, 27 (1992).
[22] R. P. Feynman, Phys. Rev. **97**, 660 (1955).
[23] G. D. Mahan, *Many-particle Physics* (Plenum, New York, 1990).
[24] S. N. Klimin and J. T. Devreese (private communication).
[25] D. Emin, Phys. Rev. B **48**, 13691 (1993).
[26] E. Kartheuser, R. Evrard, and J. Devreese, Phys. Rev. Lett. **22**, 94 (1969).
[27] J. Devreese, J. de Sitter, and M. Goovaerts, Phys. Rev. B **5**, 2367 (1972).
[28] H. G. Reik, Solid State Commun. **1**, 67 (1963).
[29] S. Fratini and S. Ciuchi, Phys. Rev. B **74**, 075101 (2006).
[30] V. V. Kabanov and D. K. Ray, Phys. Rev. B **52**, 13021 (1995).
[31] S. Ciuchi, J. Lorenzana, and C. Pierleoni, Phys. Rev. B **62**, 4426 (2000).